Factors affecting the ultrasonic intermodulation crack detection technique using bispectral analysis

Charles R. P. Courtney, Bruce W. Drinkwater *,

Simon A. Neild, Paul D. Wilcox

Department of Mechanical Engineering, University of Bristol, Queens Building, University Walk, Bristol BS8 1TR, United Kingdom

Abstract

This paper concerns the development of ultrasonic intermodulation as a method of robustly detecting cracks in engineering components. The bispectrum signal analysis processing technique is used to analyse the nonlinear response of a sample to continuous excitation at two frequencies. The increased nonlinearity due to defects such as fatigue cracks is detected. The technique is shown to be insensitive to the support conditions and excitation positions. The importance of the shape of the excited modes is demonstrated and suggests that global inspection can be achieved only by exciting multiple modes. This multi mode approach is then applied to the detection of cracking of a steel steering actuator bracket.

Key words: Inter-modulation, Non-linear, Fatigue Crack, Bispectrum

PACS: 43.35.Zc, 43.25.Dc, 43.60.Wy

1 Introduction

This paper is concerned with the development of ultrasonic intermodulation as a global method of detecting and monitoring fatigue cracks in engineering components. The ultrasonic intermodulation method makes use of the nonlinear response of cracked materials to an applied strain, by exciting the sample at a pair of frequencies and observing the resultant mixing of the signals. The work in this paper has lead to an improved understanding of the factors affecting the sensitivity of the ultrasonic intermodulation technique through a series of experiments, and progress the technique toward an industrially realisable measurement.

Fatigue cracks resulting from fluctuating stresses are a major cause of failure in engineering components and as such have attracted investigation for over a century (1). Where fatigue cannot be avoided by careful design it is necessary to undertake nondestructive testing to allow early detection of cracking and minimize the risk of failure.

The main industrial nondestructive testing (NDT) methods inspect components either by scanning (eddy current, ultrasound) or by using a wide field of view (visual inspection, magnetic particle and penetrant testing) (2), but none is global in the sense used here. A global testing technique allows a component to be tested for damage without imaging or attempting to locate the damage, the aim is to allow rapid evaluation of the state of a component with a single measurement for the whole test object. This should allow easy interpretation of the measurement and assessment of the continued viability of the

* Corresponding Author.
Email address: B.Drinkwater@bristol.ac.uk (Bruce W. Drinkwater).

component without requiring a great deal of interpretation by the operator or scanning of a measurement probe over the component. The effect of damage on the natural frequencies of a sample has been investigated as a potential global inspection technique, but this approach has been proved to be sensitive to environmental factors (3).

The large changes in nonlinear ultrasonic parameters for small degrees of damage (4; 5; 6) have stimulated interest in the use of nonlinearity for fatigue crack detection: nonlinear elastic wave spectroscopy shows promise as a route to a sensitive crack detection method. Generation of harmonics of ultrasonic signals, due to the nonlinear behavior of cracks in otherwise linear materials, was demonstrated and proposed as a crack detection technique in the late 1970s (7; 8) and continues to attract some interest for crack detection (9; 4; 10; 11; 12) and the measurement of bond strength in adhesive joints (13). At sufficiently high excitation amplitudes, subharmonics (signals with frequency content at fractions of the applied ultrasonic frequency) can be generated (14) and these are being investigated as a method of detecting closed cracks (15; 16). Donskoy *et al.* (17) demonstrated the vibroacoustic modulation technique, where a sample excited with an ultrasound signal is probed with a second low-frequency vibrational signal. When nonlinearity is present signals will appear in the response at the sum and difference of the excitation frequencies (sidebands) and these signals can be used to measure the degree of damage. Donskoy*et al.* suggested and tested two modulation methods on cracked steel pipes: impact modulation and continuous wave modulation. In each case the ultrasound signal was >100 kHz and the modulation frequency of the order of 1 kHz. Similarly Van Den Abeele *et al.* demonstrated the technique on engine connecting rods using continuous modulation of <20 kHz

and a high frequency signal of 120-134 kHz (4). Duffour *et al.* (18) performed experiments using a continuous modulation at 1 kHz, as well as experiments using impact excitation, as the low frequency excitation. The effects of varying the high frequency excitation over a wide range (50-230 kHz) and applying compressive forces to the crack were considered and a damage index, defined by results over a range of frequencies, was proposed to ensure reliable sensitivity to cracks.

Hillis *et al.* (19) used vibroacoustic modulation with two ultrasonic signals of similar order frequency (280 kHz and 462 kHz) and the same amplitude to detect cracks in steel samples. More recent work by the same group has looked at application of this technique to aircraft parts (20). The data was analysed using bispectral analysis rather than the more commonly used power-spectral analysis. Bispectral analysis is a signal processing technique (22; 23) that, due to its sensitivity to quadratic phase coupling, has attracted interest in dealing with nonlinear systems. The bispectrum was applied to a number of different non-engineering nonlinear systems before. Fackrell *et al.* (24; 25) applied it to the analysis of vibration signals and proposed its application in machine condition monitoring. Howard (26) used bispectral analysis (and trispectral analysis) to measure the coupling between frequency components in the vibration of a helicopter gearbox. More recently attempts have been made to apply bispectral analysis to crack detection problems using statistical pattern recognition applied to the bispectrum of concrete structures excited by impacts (27) or turbine blades excited by a shaker (28).

This paper starts with a short section defining the bispectrum and describing its main features before discussing the experimental setup used. The results section which follows includes experimental results relating to the dependence

of the intermodulation signal on crack length, how the sensitivity of the technique depends on the frequencies and amplitudes of the applied signals, the position of the transducers and the support conditions. A multiple mode process for applying the technique is proposed and demonstrated on a steering actuator bracket.

1.1 Bispectral Analysis

Consider a signal $x(t)$ with Fourier transform $X(f)$, where t is time and f frequency. The power spectrum is given by:

$$P(f) = E[X(f)X^*(f)] \tag{1}$$

where $E[\ldots]$ is the expectation value operator and * the complex conjugate. If the power spectrum is regarded as second order then the bispectrum is the third order given by:

$$B(f_1, f_2, f_1 + f_2) = E[X(f_1)X(f_2)X^*(f_1 + f_2)]. \tag{2}$$

Note that the third argument of B, $(f_1 + f_2)$ is dependent on the first two and so is often omitted when writing the bispectrum: $B(f_1, f_2) = B(f_1, f_2, f_1 + f_2)$. For clarity all three terms are retained here.

The bispectrum is complex and, as can be seen from equation (2), is a function of two frequencies. The behavior of the bispectrum for continuous excitation can be understood in terms of four properties required for it to be non-zero

for any pair of frequencies f_1, f_2;

$$\begin{aligned} X(f_1) &\neq 0 \\ X(f_2) &\neq 0 \\ X(f_1 + f_2) &\neq 0 \\ \varphi_3 &= \varphi_1 + \varphi_2 \end{aligned} \tag{3}$$

φ_1 and φ_2 are the phase of the signals at F_1 and F_2 respecively and φ_3 is the phase of the signal at $f_1 + f_2$. The first three conditions follow directly from equation (2) and require there is signal at the two frequencies being considered and at their sum. For cases where $\varphi_3 \neq \varphi_1 + \varphi_2$ the application of the expectation operator in equation (2) results in a zero value, but when the fourth condition in equation (3) is fulfilled non-zero values are possible(29). This phase relationship can result from second order non-linearity and is referred to as quadratic phase coupling (QPC)(29) and the bispectrum's ability to distinguish this makes it of interest in non-linear methods. It is possible to use bispectrum to remove spurious signals not caused by non-linear behaviour, although non-linear signals due sources other than damage remain a problem. The power spectrum, which discards all phase information, cannot be used to distinguish harmonically related signals which result from nonlinear interactions and those which do not.

A number of methods have been suggested for estimating the bispectrum from discrete data and a number of reviews of these techniques exist(22; 29; 30; 31). The approach used here is to average over successive records in the time domain(31). A single data set is recorded and then divided into N sections, each labelled i with the Fourier transform calculated for each section $X_i(f)$.

The bispectrum estimate is then given as:

$$B_X(f_1, f_2, f_1{+}f_2) = \frac{\sum_{i=1}^{N} X_i(f_1)X_i(f_2)X_i^*(f_1+f_2)}{N} \approx E[X(f_1)X(f_2)X^*(f_1{+}f_2)]. \tag{4}$$

The time domain signals considered in this work are voltages across PZT disks and the Fourier transforms are corrected for the window length to give the frequency domain signals also in Volts. Using Fourier transform values in volts in equation (4) gives bispectum values on Volts cubed (V^3).

2 Experimental Procedure

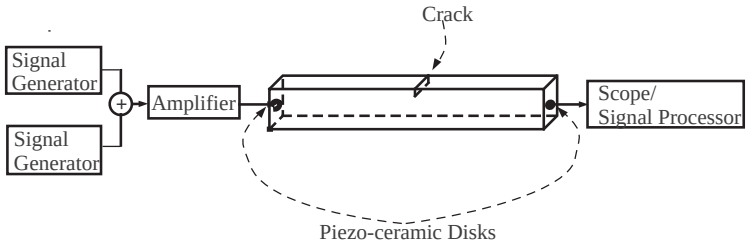

Fig. 1. Experimental Setup. Two signal generators produce sinusoidal electric signals. Signals are summed and amplified before passing to a piezoceramic disk bonded to the sample. The resulting vibration produces a signal in a second disk, which is passed to a PC for processing.

The ultrasonic intermodulation technique was applied to a series of samples with varying degrees of damage by exciting them at two frequencies and monitoring the content of the response at the difference or sum of the two applied frequencies using bispectral analysis.

Experiments were undertaken using a set of four steel beams (60 mm × 60 mm × 400 mm). One sample was undamaged, the remaining three each had

a through crack at the mid-point of one side (shown schematically in Figure 1). These cracks were of 5 mm, 15 mm and 25 mm length respectively. The samples were supported on two wires, positioned 50 mm from either end of the sample, in an effort to minimize any nonlinearity at contacts between the sample and its supports.

An excitation signal consisting of the sum of two sinusoidal signals was generated, amplified and then used to excite a 15-mm-diameter 2-mm-thick piezoceramic disk bonded to the sample under investigation using a cynoacrylate adhesive. The resulting vibration in the sample was detected by a 5-mm-diameter 2-mm-thick piezoceramic disk. The excitation frequencies were restricted to the range 100 kHz-500 kHz by the response of the piezoceramic disks. To ensure good separation of the signals due to nonlinearity, the selected frequencies were not integer multiples of each other. The continuous nature of the excitation meant that, for appropriate frequencies, standing waves were set up in the sample increasing the response. This was exploited by tuning each of the excitation frequencies to a local maximum in the frequency response of the system, corresponding to one of these vibrational modes. Having identified the appropriate frequencies the applied voltage was adjusted to set the amplitude received at each driving frequency to a predetermined level, to ensure comparability of the mixing signals between tests. The response of the detector disk to the vibration was sampled at 5 MHz digitized and passed to a PC. Each data set consisted of 500000 data points which were divided into 488 sections of 1024 points and the bispectrum estimated according to equation (4).

The process can be summarized as:

(1) Decide approximate excitation frequencies and desired amplitude in the

response.

(2) Apply first frequency to sample and tune to local maximum in sample frequency response.

(3) Adjust driving voltage to give required response amplitude at that frequency.

(4) Repeat steps 2 and 3 for second frequency.

(5) Apply both signals simultaneously to the sample.

(6) Record response for analysis offline.

3 Experimental Findings

The experiments undertaken can be broadly divided into two areas: those looking at the fundamental behavior of the sample under excitation and those investigating the effect of experimental factors. Starting with a demonstration of the principle, the fundamental experimental results will be discussed first followed by those relating to the particular experimental conditions, such as transducer position and support conditions.

3.1 Investigation of Fundamental Behavior

3.1.1 Crack Detection with Ultrasonic Intermodulation and Bispectral Analysis

To demonstrate the ultrasonic intermodulation method (previously described by Hillis et. al.(19)) each sample was excited at two vibrational modes (one at 270±2 kHz and another at 473±2 kHz) and the exciting signal adjusted so that the amplitude received at each driving frequency was 0.5 V. The

bispectrum of the response was evaluated and is shown in figure 2. In each case there are six peaks in the bispectrum, which are the only points where the bispectrum is non-zero. The two frequencies plotted are interchangeable and so the bispectrum (as plotted) is symmetrical down the line $f_1 = f_2$. Due to this symmetry the six peaks correspond to four features: the two harmonics (the peaks $B(F_1, F_1, 2F_1)$ and $B(F_2, F_2, 2F_2)$, labelled '1' and '2' respectively in figure 2) and the signals at the difference frequency ($B(F_1, F_2 - F_1, F_2)$; labelled '3') and the sum frequency ($B(F_1, F_2, F_1 + F_2)$; labelled '4'). Note that the peak due to the harmonic of the higher frequency and the peak due to the summed frequency signal rely on components of the signal that lie outside the useful frequency range of the detection system (100kHz-500kHz)

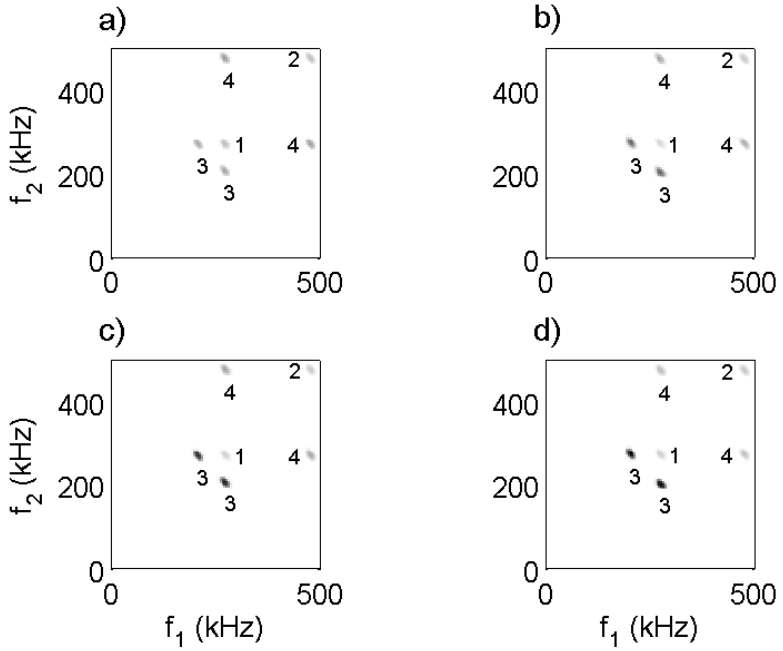

Fig. 2. Variation of Bispectrum with Crack Length. Bispectrum plots for four steel samples (60 mm × 60 mm × 400 mm), each excited at 270 kHz and 473 kHz to produce 0.5 V amplitude in the received signal at those frequencies. a) undamaged sample, and the remaining three had fatigue cracks introduced of b) 5 mm, c) 15 mm and d) 25 mm respectively. Peaks of interest are labelled 1-4.

and so are not a reliable measure of the nonlinear signal in this system.

Figure 3 shows the height of the peak $B(F_1, F_2 - F_1, F_2)$ plotted as a function of crack length for the four samples used. There is a clear progression in the peak height, with the most pronounced increase in the peak occurring between the undamaged and least damaged cases. It should be noted that there is some signal corresponding to the mixing frequency even for the undamaged sample. This is due to experimental sources of nonlinearity principally from the amplifier and the excitation transducer (it is thought that the receiving transducer introduces negligible nonlinearity due to the much lower amplitude of the received signal).

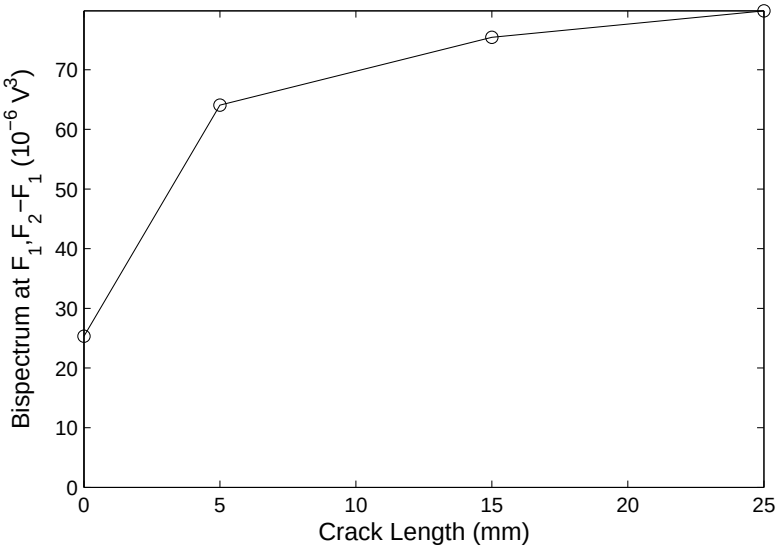

Fig. 3. Variation of Bispectrum Peak. The size of the peak $B(F_1, F_2 - F_1, F_2)$ in figure 2 is plotted against the crack length to demonstrate that ultrasonic intermodulation is sensitive to crack length

The effect of the amplifier nonlinearity has been estimated. The signal supplied by the amplifier to the transducer was recorded and the Fourier transform calculated: a small (5 mV) amplitude signal was observed at the mixing frequency (204415 Hz), compared to voltages of 4.0 V and 7.8 V at 269598 Hz and 474065

Hz (the driving frequencies). It was also found that a 50 V amplitude signal at 204415 Hz applied to the system results in a 3.6 V amplitude response. If it is assumed that the transducers and sample behave linearly, this indicates that the 5 mV inputted due to the amplifier nonlinearity corresponds to 0.4 mV in the receiver signal. Using this and the measured voltages at 269598 Hz and 474065 Hz (380 mV and 310 mV respectively) in equation 2 results in a bispectrum peak of approximately 10×10^{-6} V^3 due to the amplifier nonlinearity (a factor of eight was divided out due to the measurement of real signal amplitudes, but the use of Fourier coefficients in equation 2). The bispectrum peak measured for the undamaged case was $25 \times 10^{-6} V^3$. This suggests that the amplifier is one of the main causes of this nonlinearity. Separating the two excitations, by using a separate amplifier and transducer for each applied frequency, is a potential method of reducing the nonlinear effect of the amplifier and transducer and ensuring that all mixing occurs in the sample, although at the cost of some increase in experimental complexity and equipment. Tests using two amplifiers and two transducers indicate a moderate (approximately 20%) reduction in the mixing signal for the undamaged sample (21). For samples requiring similar (or lower) levels of excitation to those considered in this paper, the single amplifier and transducer configuration is both adequate and experimentally simple. For particularly difficult-to-excite samples, or where this configuration is not sufficiently sensitive, using separate amplifiers and transducers may offer a solution. A test of the effect of the transducer-sample contact on the nonlinearity is included in the next section.

3.1.2 Amplitude and Frequency Dependence

The signal used for the excitation of the system can be characterized by three parameters: the two frequencies used and the amplitude of the response at each of these frequencies (as only the case where applied voltage is adjusted to give the same response voltage for both frequencies is considered here). In order to investigate how these parameters affect the sensitivity of the technique to damage the undamaged sample and the sample with the 25 mm crack were used.

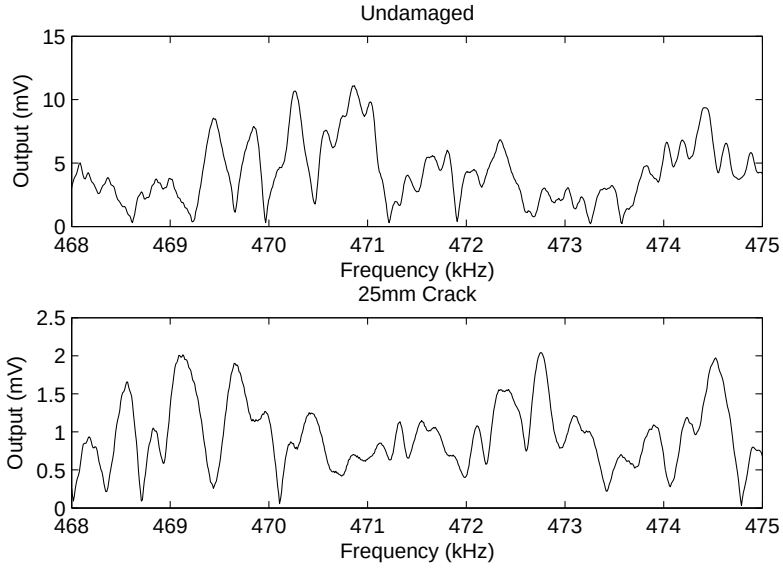

Fig. 4. Response of a) undamaged and b) 25-mm-cracked samples to a slowly swept excitation signal. Excitation frequency was swept from 468 kHz to 475 kHz whilst maintaining constant excitation voltage amplitude (20 V).

The implementation of ultrasonic intermodulation uses frequencies selected to correspond to local maxima of the sample response. Figure 4 shows the response of the samples excited by a slowly swept signal running from 468 kHz to 475 kHz at constant input amplitude over 100ms. The plot indicates how high the modal density is and the number of possible choices of frequency

Table 1

Mean $B(F_1, F_2 - F_1, F_2)$ values for 160 mV response at each frequency. Effect of removing and replacing transducer.

$B(F_1, F_2 - F_1, F_2) \times 10^6 V^3$ at 160 mV	
Mean	St. Dev.
0.5	0.4
0.7	0.4
0.4	0.1
3.1	1.3

available, even over such a narrow range. The modal structure is different in the two cases and so there is no guarantee that the same mode, with the same mode shape, can be selected in each case. Behavior is similar in the region around 270 kHz. Figure 5 shows the effect of applying the ultrasonic intermodulation technique to a large number of modes in the region 468-475 kHz and a fixed lower excitation frequency corresponding to the strongest response in the region 269-271 kHz (270693 Hz for the undamaged sample and 269243 Hz for the cracked sample). The applied voltage at each of frequency pair was changed for each measurement, such that the responses at F_1 and F_2 remained equal to each other and increased from 10mV to 200mV over 20 measurements per pair. Although results for the damaged and undamaged case clearly differ, each set of results varies widely with the upper frequency used. This indicates that, if only a single pair of modes is used, for some choices of modes the ability to detect a crack is reduced.

The mean value (averaged over all the modes shown) of each data set is plotted

alongside the individual mode results (indicated with dots). For comparison, with a 160 mV response at the driving frequencies, the mean for the undamaged specimen was 0.7×10^{-6} V^3 with a standard deviation of 0.4×10^{-6} V^3 and for the 25-mm-cracked specimen 14.0×10^{-6} V^3 with a standard deviation of 4.5×10^{-6} V^3. The nonlinearity of the amplifier was identified, in section 3.1.1, as a major source of experimental nonlinearity for undamaged samples. The contact between the input transducer and the sample was another potential source of nonlinearity and so the transducer used on the undamaged sample was removed, replaced and the experiment repeated. This was done a total of four times and the results are shown in table 1. As can be seen there is some variation in the average value; the final result is somewhat higher than the others, however it does not approach the value obtained for the damaged sample.

Figure 6 shows the increase in the bispectrum peak $B(F_1, F_2 - F_1, F_2)$ with increasing vibration at a given pair of driving frequencies on a log-log plot. The damaged sample results follow the power law $B(F_1, F_2 - F_1, F_2) \propto X^{\beta}(F_i)$ where $X(F_i) = X(F_1) = X(F_2)$. Least-squares fitting to the data in figure 6 gives an average (over all the considered modes) gradient of $\beta = 3.97$ (standard deviation, 0.11) for the cracked sample. $\beta = 4$ for a quadratic nonlinearity(19). The undamaged sample undergoes a shift in gradient in figure 6 at approximately 50 mV amplitude (-1.3 on the log scale) at each driving frequency: below this value the average gradient, $\beta = 2.27$ (standard deviation, 0.26) and above the gradient, $\beta = 3.70$ (standard deviation, 0.34). From equation 2 it can be seen that a constant value of the amplitude at the difference signal will lead to $\beta = 2$. A value of $\beta = 2$ would be expected if the only signal, $X(F_2 - F_1)$, were a noise unrelated to the excitation amplitude. The behavior

of the undamaged sample suggests that there is a small source of nonlinearity that is initially smaller than a noise floor, but exceeds this level once the linear response at the excitation frequencies exceeds 50 mV, whereas in the damaged sample the amplitude-dependent nonlinear signal exceeds the static noise value at all excitation amplitudes considered.

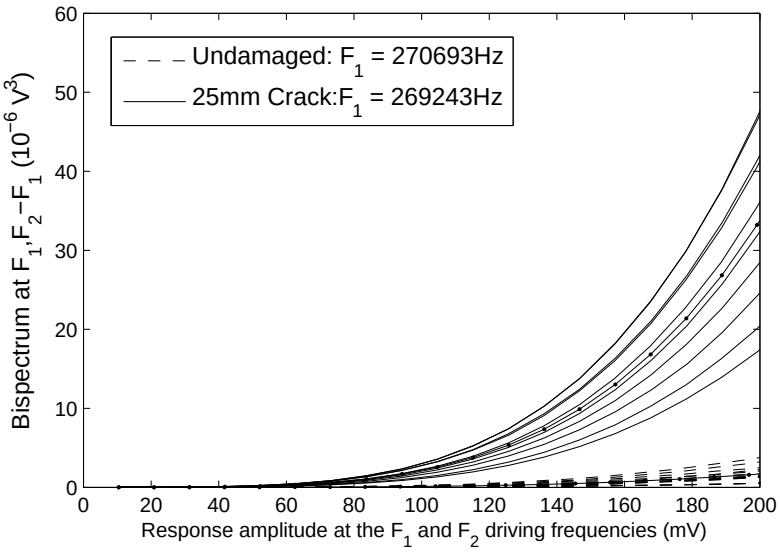

Fig. 5. Effect of mode selection and vibration amplitude on ultrasonic intermodulation signals. Local maxima in the frequency response of the samples in the region 468-475 kHz were identified and intermodulation measurements made for each. The bispectrum peaks $B(F_1, F_2 - F_1, F_2)$ are plotted as a function of amplitude for all the modes selected for the undamaged (dashed line) and 25-mm-cracked (solid line) samples. The average over each set of modes is shown as a solid line with dots.

So far the results have been performed for a particular lower frequency vibrational state. Repeating the experiments, using the same transducer, for another three low frequencies (F_1 = 269243 Hz, 269396 Hz and 270540 Hz) produces some variation in the average value of $B(F_1, F_2 - F_1, F_2)$ over the same set of F_2 each time at 160 mV amplitude. The average over the F_2 frequency range for the undamaged sample varies from 0.4 to 8 $\times 10^{-6} V^3$ de-

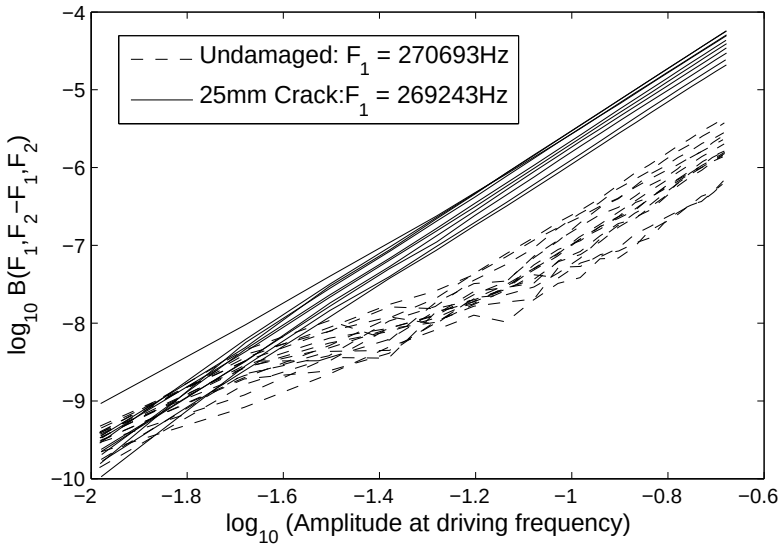

Fig. 6. Effect of mode selection and vibration amplitude on ultrasonic intermodulation signals. The same data shown in figure5 is plotted on a log-log scale to demonstrate the power law relationship between signal amplitude at the driving frequencies and the nonlinear signal

pending on the F_1 value used. This reflects the selection of modes with poorer transfer of motion between the input and output transducers than the original selections, requiring higher applied voltages and so more nonlinear signal from the amplifier and transducer.

3.1.3 Modal Response

In order to investigate the effect of the selected mode further, the intermodulation experiment was performed with a response amplitude of 0.5 V at each excitation frequency, with F_1 fixed and F_2 corresponding to each of the vibrational modes in the region 468-475 kHz. Figure 7 shows the resulting bispectrum signal $B(F_1, F_2 - F_1, F_2)$ against the frequency of the higher mode (the lower frequency, F_1, remains at 271960 Hz throughout). As in figure 5 there is a wide spread of response with frequency for a given excitation amplitude

and there is no apparent correlation between the response and the frequency.

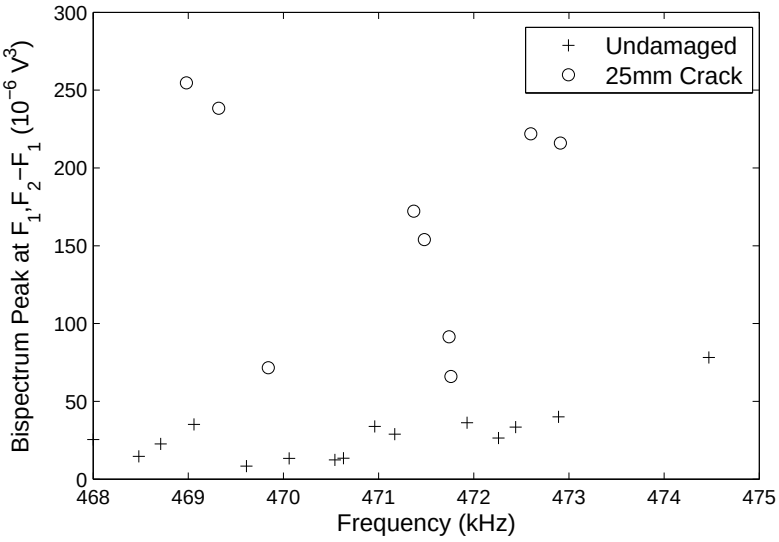

Fig. 7. Variation of nonlinearity with mode selected. Samples excited at fixed lower frequency (F_1 = 271900 Hz) excitation and upper frequencies from F_2 =468 kHz to F_2 =475 kHz and excitation adjusted to give 0.5 V amplitude in the response at each driving frequency.

A third piezoceramic disk was added at the midpoint of one (long) side 5 mm from the edge, such that it was positioned across the crack of the 25 mm sample and at an equivalent position of the undamaged sample. Figure 8 shows the bispectrum response, $B(F_1, F_2 - F_1, F_2)$, against the peak-to-peak voltage across the piezoceramic disk at the crack. The response amplitude at the crack at F_1 (which was fixed) was 0.1 V for all the measurements. The response amplitude at F_2 at the crack varied from 0.03 V to 0.3 V (depending on the F_2 value used). This results in the peak-to-peak response variation from 0.26 to 0.8 V seen in figure 8. From figure 8 it is clear that the mixing signal generated by the system for a given vibration detected at the end point, remote from the crack, depends on the level of vibration at the crack with a response very close to the undamaged behavior for the lowest signals at the crack, increasing

sharply as the level of vibration increases before flattening at approximately $250 \times 10^{-6} V^3$. There is no clear relationship between the response at the crack position transducer and the bispectrum peak for the undamaged sample, as would be expected. This result demonstrates the importance of exciting the crack sufficiently at both frequencies to get the required mixing and the large difference in the excitation at a particular point that occurs for different vibrational modes that are very similar in frequency. This presents a difficulty in using the ultrasonic intermodulation with continuous excitation as great care must be taken to ensure that the same mode is selected for each measurement when a comparison is to be made and for any given mode pair there will always be regions that are not excited at one or other frequency resulting in blind spots for the technique. This suggests that to properly test an object multiple modes should be used, either simultaneously using broadband excitation or concurrently by making multiple measurements using pairs of continuous signals at different frequencies. From the averages plotted in figure 5 it appears that taking a straightforward average over a range of modes for a given response amplitude at each of the driven modes offers a straightforward solution although both modes would need to be varied rather than just the one as in section 3.1.2. The importance of mode shape and selection to detection sensitivity has also been an area of interest in the use of guided waves for defect detection(32). There the solution is often appropriate selection of a single mode(33; 34), although multimode approaches have been applied(35; 36).

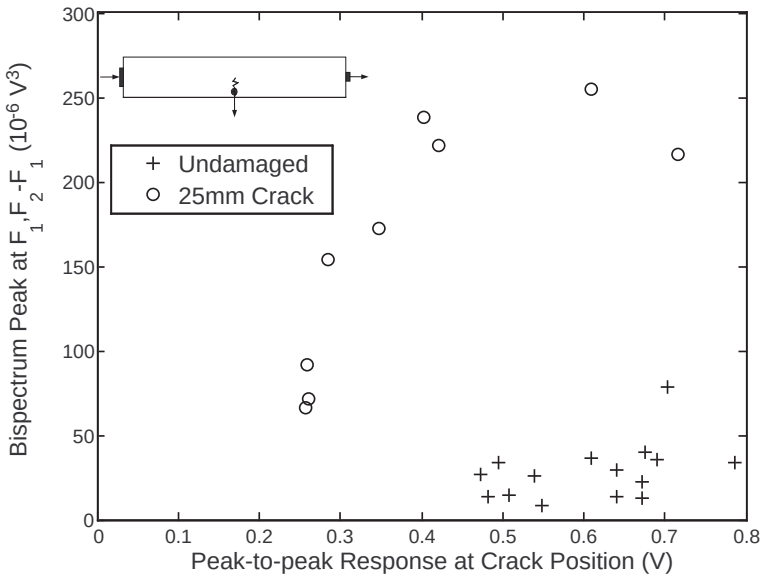

Fig. 8. Variation of mixing signal with vibration at crack. Result shown in 7 plotted against peak-to-peak voltage across piezoceramic disk positioned at crack (or equivalent position on undamaged sample) as shown schematically in inset.

3.2 Experimental Factors

In addition to the amplitude and frequency of the signal applied to the system there are other experimental factors that need to be considered when using the ultrasonic intermodulation technique. Experiments have been undertaken to evaluate the importance of the positions of the transducers used for excitation and reception and the support conditions of the sample.

3.2.1 Excitation Positions

The samples were excited, as previously, with two sinusoidal frequencies tuned to vibrational modes and with the exciting signal adjusted so that the amplitude received at each driving frequency was 0.5 V. Figure 9 shows the resulting bispectrum mixing peaks as a function of crack length for three transducer

configurations, via transducers located at the ends of the sample (as used previously), and two configurations with the transducers on the same side of the sample as the crack: one with the transducers 40 mm from the ends (so that the crack falls between them) and one with the driving transducer 40 mm from one end and the receiving 80 mm from the same end. The configurations are shown schematically, with the results in figure 9. Note that due to difficulty reaching a sufficient level of excitation the configuration using two close (40 mm separation) transducers was performed with $F_1 = 270 \pm 2$ kHz and $F_2 = 440 \pm 2$ kHz rather than $F_1 = 270 \pm 2$ kHz and $F_2 = 473 \pm 2$ kHz as with the other two setups.

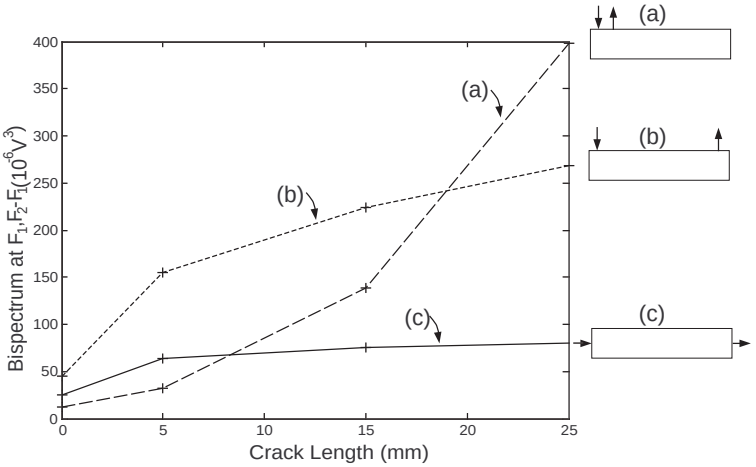

Fig. 9. Effect of varying transducer position. Bispectrum peak, $B(F_1, F_2 - F_1, F_2)$, as a function of crack length for three different transducer configurations a) top of sample 40 mm separation, b) top of sample 320 mm separation and c) opposite ends.

Figure 9 shows that for each configuration there is a clear progression in the signal due to the crack nonlinearity. The two configurations where the transducers are either side of the crack are similar in behavior with a large increase in signal between the undamaged and 5-mm-cracked states with a slow increase as the crack grows. The configuration with two transducers closely

separated differs in that the rate of increase grows for longer cracks. It should be noted that the contrast between no-crack and the smallest crack is similar for all the configurations. The large variations in response due to the use of different modes shown in figures 4, 5, 7 and 8 indicate that the variations in behavior shown in figure 9 could be explained by inconsistent selection of mode across the different samples.

3.2.2 Support Conditions

The support conditions used for all the preceding experiments (suspension by two wires) were intended to minimize the possibility of sample-support contacts resulting in nonlinearities. The necessity of these precautions was tested by measuring the mixing signal produced when the undamaged sample was clamped at one end with a force that was varied from 300 N to 10,000 N applied over $3 \times 10^{-3}\text{m}^2$ leading to pressure of 100 kN/m^2 to 3 MN/m^2. The nonlinear behavior of cracks is understood as originating from the varying degree of contact between the crack surfaces during the induced vibration (14; 17). In principle it would be expected that any two metal surfaces (including the sample-clamp interface) in contact could exhibit similar behavior resulting in increased nonlinear signals even for the undamaged sample when compared to experiments undertaken (as in previous sections) with supports designed to avoid metal-metal contacts.

The sample was excited such that the received signal at each driving frequency was 160 mV and the bispectrum peak $B(F_1, F_2 - F_1, F_2)$ calculated. This was repeated using excitation modes across the regions F_1 =270 kHz to 273 kHz and F_2 =469 kHz to 473 kHz. Figure 10 shows the results for the sample

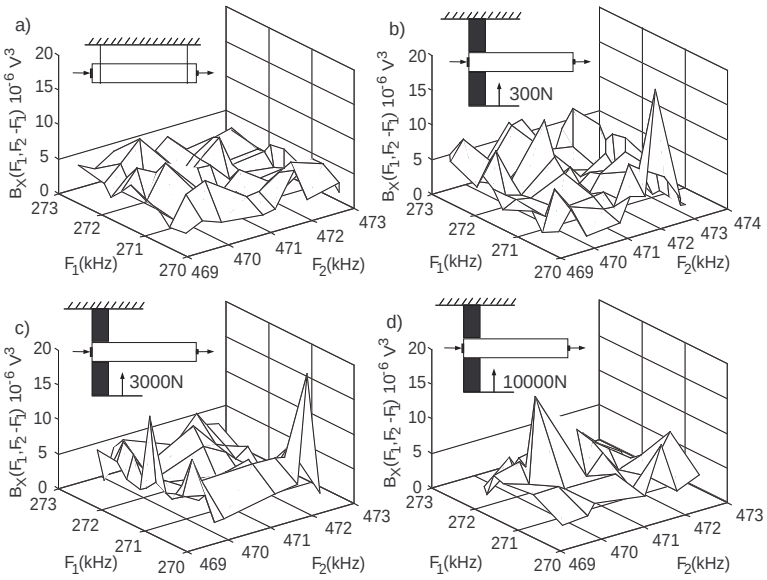

Fig. 10. Effect of Supoort Conduitions on Mixing Signal. The Bispectrum peak, $B(F_1, F_2 - F_1, F_2)$, for all possible pairs of modes in the regions F_1 =270 kHz to 273 kHz and F_2 =469 kHz to 473 kHz excited to give 160 mV at each frequency in the response. a) suspended the sample on wires as in all the previous experiments b), c) and d) clamped the sample at one end with forces of 300N, 3000N and 10000N respectively.

suspended on wires (as previously) and clamped at one end (as shown in the figure) with a force of 300 N, 3000 N and 10,000 N over an area of $3 \times 10^{-3}\text{m}^2$. The behavior is similar for all the tested mode combinations. Figure 11 shows the effect on the average peak value, over the frequency ranges considered, with increasing force applied to the clamps. The average value for the suspended sample is included for comparison. There is a small increase in the average peak size when the sample is clamped rather than suspended, but this does not appear to be clearly dependent on the force applied. The increase in the nonlinear signal between the suspended sample and the clamped samples is small when compared to the increases found earlier between an undamaged sample and a 25-mm-cracked sample. Buck et. al. (7) showed that for a pair of alu-

minium samples compressed together, the contact introduced nonlinearity at low compression forces, but that the nonlinear behavior (measured as the harmonics produced when the system was excited by a 5 MHz longitudinal wave) decreased rapidly with increasing pressure before asymptotically approaching the value found for a glycerine filled crack. Similar behavior was observed by Brotherhood et. al. using 1.85 MHz excitation to detect the first harmonic produced at a kissing bonds in adhesive joints between two aluminium samples (37) with the harmonic amplitude approaching that found for a perfect crack. The lack of variation in nonlinear response with increased force in the results shown in figure 11 suggest that the pressures applied here are sufficient that the clamp-sample contact behaves in an approximately linear manner.

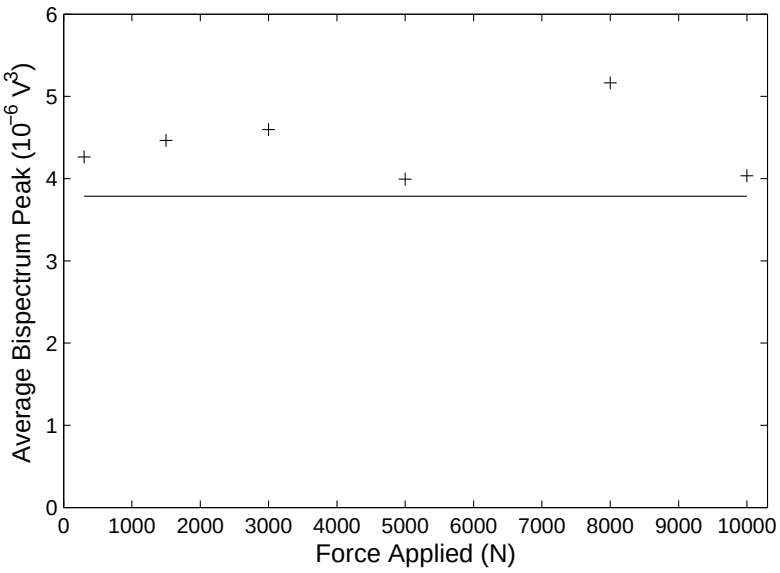

Fig. 11. Average Bispectrum Peak with Increasing Clamping Force. Bispectrum peak $B(F_1, F_2 - F_1, F_2)$ averaged over all pairs of the vibrational modes for F_1 =270 kHz to 273 kHz and F_2 =469 kHz to 473 kHz. The horizontal line shows the same average for the sample suspended by wires for comparison.

4 Multiple Mode Method

The method of performing measurements for combinations of modes from two frequency regions, used in section 3.2.2, was applied to a real aeronautical part (a steering actuator bracket) with an artificially grown fatigue crack to demonstrate its use to detect damage in engineering components. First there is a more precise outline of the proposed method, followed by a description of the sample and the results associated.

4.1 Proposed Method

The approach proposed, in order to apply the inter-modulation technique whilst removing the difficulties due to the sensitivity of the response to the modes selected, is to identify all the modes in two frequency regions and analyse the response of the sample as all combinations of one low and one high frequency. The approach for each pair is the same as described in section 2. Modes are identified by measuring the response of the sample to a slowly swept signal, with local maxima in the response giving the modal frequencies.

(1) Choose excitation frequency ranges and desired amplitude in the response.
(2) Apply signal swept across first frequency range and record response.
(3) Perform Fourier transform and locate local maxima in response.
(4) Repeat steps 2 and 3 for second frequency range.
(5) Select one pair of modes and apply sinusoidal signals at those frequencies.
(6) Adjust input to give desired response at each mode.

(7) Repeat steps 5 and 6 for each combination of modes.

(8) Evaluate mixing signal at each pair.

(9) Use statistical measure of peaks over all pairs to evaluate damage.

4.2 Steering Actuator Bracket

A pair of steering actuator brackets from a Let L410 commuter aircraft were supplied to us by the Czech Aeronautical Research and Test Institute (VZLU)one undamaged and one that has been artificially fatigued, resulting in a crack at the critical point (marked on figure 12) perpendicular to the surface, with a visible length of 9mm and depth of 3mm, constituting approximately 10-15% of the cross-sectional area (the sample has a 12mm by 15mm cross-section at the critical point). Figure 12 shows the shape of the steering actuator bracket along with the positions of for piezoceramic disks (labelled A-D) bonded to it. All the disks were 5-mm-diameter 2-mm-thick disks bonded with cyanoacrylate adhesive.

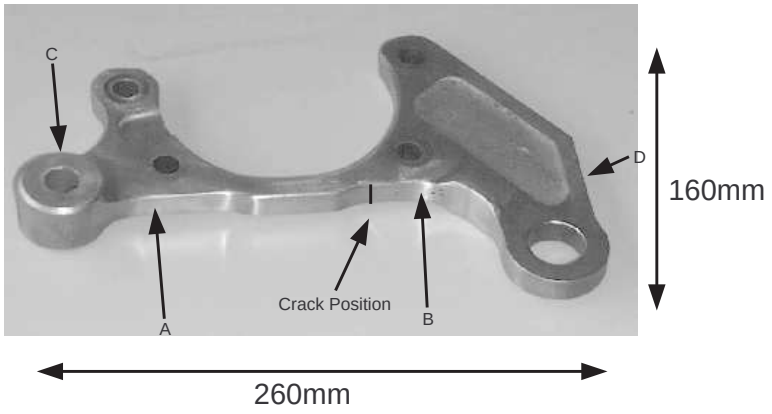

Fig. 12. Steering Actuator Bracket from a Let L410 commuter aircraft with transducer positions labelled A-D. Sample provided by Aeronautical Research and Test Institute (VZLU), Prague

Initially disk A was used for excitation of the sample and disk B to record the response. The lower excitation frequencies (F_1) were the local maxima in the response of the sample to a swept signal from 270kHz to 272KHz, and the higher excitation frequencies (F_2) were in the region 472 kHz to 474 kHz. There were 9 modes in the lower region and 7 in the upper, leading to a total of 63 pairs. At each of these pairs the excitation amplitudes were adjusted to give a response of 100mV at each of the two excitation frequencies. The resulting response at disk B was recorded and the bispectrum calculated. Figure 13 shows the peak $B(F_1, F_2 - F_1, F_2)$ for both the damaged and undamaged samples plotted both as a function of the exciting frequencies and also as a distribution of peak values over each set of mode pairs. There is a broad spread of results for both damaged and undamaged samples, but the damaged case has more high values and a higher maximum. The undamaged bracket results in a mean peak of 1.3×10^{-6} V^3 with a standard deviation of 1.7×10^{-6} V^3, testing the damaged sample gives a mean of 3.7×10^{-6} V^3 with a standard deviation of 3.2×10^{-6} V^3. Table 2 shows the same process repeated for three other transducer pairs and lists the mean, standard deviation and spread of values for each set of results. In each case there is an overlap in the spreads between the damaged and undamaged cases, reiterating that use of single pairs of modes is likely to be unreliable, but in each case there is a clear difference between the mean values and the standard deviations when the bracket contains damage compared to the undamaged case. The choice of the mean represents a viable and straightforward statistical measure of the increased non-linearity, more elaborate measures may also present a method of improving the method, in particular the use of the average removes any spatial information that could be obtained from the mode shapes. Although it would require a very good understanding of the modes of the sample, in principle it

should be possible to use some weighting method to extract information about the position of the damage from the variation of the response with mode shape, this lies outside the scope of this paper which explores the development of a global technique for damage detection.

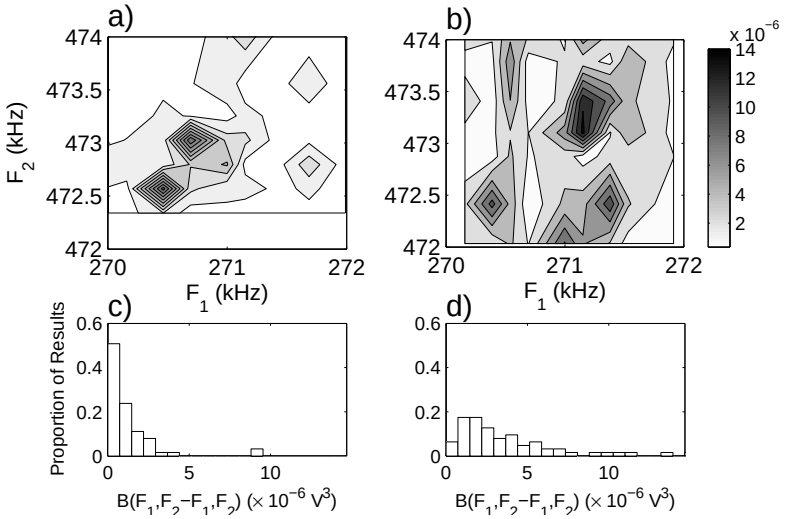

Fig. 13. Response of Steering Actuator Brackets to Ultrasonic Intermodulation. Bispectrum peak, $B(F_1, F_2 - F_1, F_2)$ plotted for each pair of excitation frequencies corresponding to modes in the regions 270-272 kHz (F_1) and 472-474 kHz (F_2). Contour plots (a and b) show bispectrum peak as function of two excitation frequencies and histograms (c and d) show distribution of peak heights for each data set. Results on left (a and c) are for undamaged bracket and on right (b and d) for a bracket with a fatigue crack introduced.

5 Conclusions

This paper has investigated the factors affecting the mixing signal produced by a damaged sample continuously excited at two vibrational modes, with a view to stimulating progress towards a practical application to the technique.

The bispectrum was used to analyse the response of the excited sample. The

Table 2

Statistical Measures of Response of Steering Actuator Bracket to Two Frequency Excitation

Transducers		Undamaged Response ($\times 10^{-6} V^3$)			Damaged Response ($\times 10^{-6} V^3$)		
Excitation	Response	Mean	Standard Deviation	Spread	Mean	Standard Deviation	Spread
A	B	1.3	1.6	0.1-9.5	3.5	3.2	0.3-14.7
A	D	2.9	2.8	0.2-10.6	5.2	4.7	0.4-27.1
B	C	0.9	0.9	0.1-4.5	3.7	3.6	0.4-16.7
C	D	2.1	1.8	0.1-9.4	3.4	2.5	0.2-9.8

signal at the difference of the exciting frequencies was monitored and was shown to be increased by the presence of damage. The technique was found to be robust with regards the transducer position and the boundary conditions and valid over a range of vibrational amplitudes (for a given frequency pair). The key finding regarding the application of the technique was found to be the level of vibration at the crack, which depends on the shape of the modes selected. For experiments relying on a single pair of modes this makes the method unduly fragile. A method that excites a number of modes, either during one test or a series of consecutive tests, would remove the possibility that a particular mode had been selected with a node positioned at the damage. Such a method has been proposed and demonstrated on a geometrically complex engineering part.

6 Acknowledgements

This work was funded as part of the European Union specific targeted research project AERONEWS (AST-CT-2003-502927).

References

[1] W. Schütz, A history of fatigue, Engineering Fracture Mechanics 54 (1996) 263–300.

[2] P. Cawley, Non-destructive testingcurrent capabilities and future directions, Proceedings of the Institution of Mechanical Engineers, L 215 (2001) 213–223.

[3] O. S. Salawu, Detection of structural damage through changes in frequency: A review, Engineering Structures 9 (1997) 718–723.

[4] K. E.-A. V. D. Abeele, A. Sutin, J. Carmeliet, P. A. Johnson, Micro-damage diagnostics using nonlinear elastic wave spectroscopy (news), NDT&E International 34 (2001) 239–248.

[5] P. B. Nagy, Fatigue damage assessment by nonlinear ultrasonic materials characterisation, Ultrasonics 36 (1998) 375–381.

[6] V. Zaitsev, P. Sas, Nonlinear response of a weakly damaged metal sample: A dissipative modulation mechanism of vibro-acoustic interaction, Journal of Vibration and Control 6 (2000) 803–822.

[7] O. Buck, W. L. Morris, J. M. Richardson, Acoustic harmonic generation at unbonded interfaces and fatigue cracks, Applied Physics Letters 33 (1978) 371–373.

[8] W. L. M. O. Buck, R.V.Inman, Acoustic harmonic generation due to

fatige damage in high-strength aluminium, Journal of Applied Physics 50 (1979) 6737–6741.

[9] I. Y. Solodov, Ultrasonics of non-linear contacts: Propagation, reflection and nde-applications, Ultrasonics 36 (1998) 383–390.

[10] C. Pecorari, Nonlinear interaction of plane ultrasonic waves with an interface between rough surfaces in contact, Journal of the Acoustical Society of America 113 (2003) 3065–3072.

[11] J. Y. Kim, V. A. Yakovlev, S. I. Rokhlin, Parametric modulation mechanism of surface acoustic wave on a partially closed crack, Applied Physics Letters 82 (2003) 3203–3205.

[12] J. Y. Kim, V. A. Yakovlev, S. I. Rokhlin, Surface acoustic wave modulation on a partially closed fatigue crack, Journal of the Acoustical Society of America 115 (2004) 1961–1972.

[13] S. Hirsekorn, Nonlinear transfer of ultrasound by adhesive joints a theoretical description, Ultrasonics 39 (2001) 57–68.

[14] I. Y. Solodov, B. A. Korshak, Instability, chaos, and "memory" in acoustic-wave crack interaction, Physical Review Letters 88 (2002) Art. No. 014303.

[15] K. Yamanaka, T. Mihara, T. Tsuji, Evaluation of closed cracks by analysis of subharmonic ultrasound, Insight 46 (2004) 666–670.

[16] Y. Ohara, T. Mihara, K. Yamanaka, Effect of adhesion force between crack planes on subharmonic and dc responses in nonlinear ultrasound, Ultrasonics 44 (2006) 194–199.

[17] D. Donskoy, A. Sutin, A. Ekimov, Nonlinear acoustic interaction on contact interfaces and its use for nondestructive testing, NDT&E International 34 (2001) 231–238.

[18] P. Duffour, M. Morbidini, P. Cawley, A study of the vibro-acoustic mod-

ulation technique for the detection of cracks in metals, Journal of the Acoustical Society of America 119 (2006) 1463–1475.

[19] A. J. Hillis, S. A. Neild, B. W. Drinkwater, P. D. Wilcox, Global crack detection using bispectral analysis, Proceedings of Royal Society 462 (2006) 1515–1530.

[20] C. R. P. Courtney, B. W. Drinkwater, S. A. Neild, P. D. Wilcox, Global crack detection using bispectral analysis, in: ECNDT, 2006, proceedings of the 9th European Non Destructive Testing Conference.

[21] C. R. P. Courtney, B. W. Drinkwater, S. A. Neild, P. D. Wilcox, Ultrasonic intermodulation for global non-destructive testing, in: ICA, 2007, proceedings of the 19th International Congress on Acoustics.

[22] C. L. Nikias, M. R. Raghuveer, Bispectrum estimation: A digital signal processing framework, Proceedings of the IEEE 75 (1987) 869–891.

[23] W. B. Collis, P. R. White, J. K. Hammond, Higher-order spectra: The bispectrum and trispectrum, Mechanical Systems and Signal Processing 12 (1998) 375–394.

[24] J. W. A. Fackrell, P. R. White, J. K. Hammond, R. J. Pinnington, The interpretation of the bispectra of vibration signals-i. theory, Mechanical Systems and Signal Processing 9 (1995) 257–266.

[25] J. W. A. Fackrell, P. R. White, J. K. Hammond, R. J. Pinnington, The interpretation of the bispectra of vibration signals-ii. experimental results and applications, Mechanical Systems and Signal Processing 9 (1995) 257–266.

[26] I. M. Howard, Higher-order spectral techniques for machine vibration condition monitoring, Proceedings of the Institution of Mechanical Engineers, G 211 (1997) 211–219.

[27] Y. Xiang, S. K. Tso, Detection and classification of flaws in concrete

structure using bispectra and neural networks, NDT&E International 35 (2001) 19–27.

[28] L. Gelman, P. White, J. Hammond, Fatigue crack diagnostics: A comparison of the use of complex bicoherence and its magnitude, Mechanical Systems and Signal Processing 19 (2005) 913–918.

[29] M. R. Raghuveer, C. L. Nikias, Bispectrum estimation: A parametric approach, IEEE Transaction on Acoustics, Speech, and Signal Processing ASSP13 (1985) 1213–1230.

[30] M. RosenBlatt, Estimation of the bispectrum, The Annals of Mathematical Statistics 36 (1965) 1120–1136.

[31] P. J. Huber, B. Kleiner, T. Gasser, Statistical methods for investigating phase relations in stationary stochastic processes, IEEE Transaction on Audio and Electroacoustics AU19 (1971) 78–86.

[32] J. J. Ditri, J. L. Rose, G. Chen, Mode selection criteria for defect optimization using lamb waves, in: D. O. Thompson, D. E. Chimenti (Eds.), Review of Progress in Quantitative Nondestructive Evaluation, 1992, proceedings of the 18th Annual Review of Progress in Quantitative Nondestructive Evaluation.

[33] M. Lowe, D. Alleyne, P. Cawley, Defect detection in pipes using guided waves, Ultrasonics 36 (1998) 147–154.

[34] J. L. Rose, Guided wave nuances for ultrasonic nondestructive evaluation, IEEE Transaction on Ultrasonics, Ferroelectrics, and Frequency Control 47 (2000) 575–583.

[35] J. Hou, K. R. Leonard, M. K. Hinders, Automatic multi-mode lamb wave arrival time extraction for improved tomographic reconstruction, Inverse Problems 20 (2004) 1873–1888.

[36] O. Kotte, M. Niethammer, L. J. Jacobs, Lamb wave characterization by

differential reassignment and non-linear anisotropic diffusion, NDT&E International 39 (2006) 96–105.

[37] C. J. Brotherhood, B. W. Drinkwater, S. Dixon, The detectability of kissing bond in adhesive joints using ultrasonic techniques, Ultrasonics 41 (2003) 521–529.